

Preparation of Sulfonated Polypropylene and Its Dyeability: Thiol as a Functionalization Template of Polypropylene

Yeon Beom Choi, O Ok Park

Department of Chemical and Biomolecular Engineering, Brain Korea 21 Graduate Program of Korea, Advanced Institute of Science and Technology, 373-1 Guseong-dong, Yuseong-gu, Daejeon 305-701, Republic of Korea

Received 18 October 2007; accepted 19 January 2008

DOI 10.1002/app.28054

Published online 7 April 2008 in Wiley InterScience (www.interscience.wiley.com).

ABSTRACT: A two-step process has been invented to prepare sulfonated polypropylene from chlorinated polypropylene via thiolation and successive oxidation to enhance the dyeability of polypropylene. With a short thiolation reaction time of 3 h in an *N*-methyl-2-pyrrolidone solution, 1.7–20.5% sulfur can be incorporated into a polypropylene bulk effectively. Chlorine–thiol substitution and hydrosulfide conversion have been examined with elemental analysis, and their behaviors as a function of the SH/Cl ratio can be explained with an equilibrium model of hydrosulfide and accessible chlorine in a given timescale. Oxidation of thiol has been performed successfully with hydrogen peroxide. The evolution of oxidation intermedi-

ates such as sulfoxide, sulfone, sulfinic acid, and sulfonic acid can be identified by Raman and Fourier transform infrared analyses. Sulfonated polypropylene can be stained by a basic dye very effectively, and its dye uptake reaches 190 mmol of dye/kg of polymer for 3.6 mmol of sulfur/g of polymer. This dye uptake is 20 times more effective than that of chlorinated polypropylene on a molar basis. Thus, it is clear that a modification can be performed effectively to enhance the dyeability of polypropylene. © 2008 Wiley Periodicals, Inc. *J Appl Polym Sci* 109: 736–748, 2008

Key words: dyes/pigments; FTIR; functionalization of polymers; poly(propylene) (PP); Raman spectroscopy

INTRODUCTION

Polypropylene (PP) has many advantages among general-purpose polymers, including its relatively low price, nontoxicity, good mechanical properties, recyclability, and resistance to many chemicals. Thus, its range of applications extends to packaging, appliances, fibers, and automotive and industrial fields. Conversely, PP does not have a specific functional group. Its lack of chemical affinity limits its use in applications such as coating, printing, coloring, and adhesion to other materials. In particular, the improvement of its dyeability is an interesting challenge in the area of PP research. PP fibers are difficult to dye by conventional dyeing processes, most of which involve a mass coloration technique in which a master batch of colorant is mixed with normal chips and they are processed together.¹ The master-batch technique is convenient and highly productive and provides savings in cost. However, this process is not always economical for coloring small lots in different shades and lacks flexibility.

The cleaning of processing units is required for any change in color, and this is a very time-consuming operation. The choice of colorants is limited to non-volatile, thermally stable pigments for high processing temperatures. In a field in which consumers' needs are rapidly changing, a well-developed conventional dyeing technique can offer more flexibility to the dyer if PP is dyeable.

The basic concept of dyeable PP is related to the introduction of functional groups that can provide specific interactions between dyes and PP. Several studies have been conducted on preparing polymer blends with a range of other polymers as dye-accepting sources because of their inherent dyeability; these have provided functional groups such as acrylate,^{2,3} amide,⁴ alkyl amine,⁵ pyridine,⁶ ester,⁷ acetate,⁸ and organoclay.⁹

The key problem of polymer blends is the trade-off relationship between compatibility with PP and affinity to the dye. Ideally, it is preferable that the dye-accepting sites are distributed evenly throughout the PP matrix. However, polymers having good compatibility with PP are associated with low polarity, which implies a lack of affinity. In contrast, good affinity to a dye implies that a polymer has a functional group that will provide a strong interaction with the dye in a manner different from van der Waals interactions. This will accelerate the blooming

Correspondence to: O O. Park (ookpark@kaist.ac.kr).

Contract grant sponsors: Samsung Total Petrochemicals, Brain Korea 21 Program.

or phase separation of the dispersed phase and will eventually fail to achieve a fine quality of staining. The other feature of the blending approach is the limitation in dyeability. The dyeability depends on the inherent property of the blended polymer; the maximum dye uptake cannot exceed that of the blended polymer.

Regarding dyeability, grafts,^{10–12} surface activation techniques such as e-beam, UV, glow discharge plasma, and ozone, and combinations of these methods^{13–19} may be more effective than blends, as they are directly introducing polar moieties into the PP chain and are free from phase separation. Activation of the surface by chemicals is another method of creating dye sites.²⁰ Chlorination^{21,22} and oxidation²³ have also been studied in an effort to improve the dyeability of PP.

These grafting and surface modifications have notable shortcomings. Because of the lack of solubility of PP, reactions on PP are performed under heterogeneous conditions, and modifications can reach only the surface of the PP films or fibers. In terms of dyeing applications, the dye molecules bound onto the surface are easily torn off by environmental stressors; therefore, it is fair to say that bulk modification is certainly necessary for enhanced resistance of the bound dye molecules to any physical or chemical attack. Moreover, although the surface can be modified intensively, the total quantity of incorporated functional groups can be small in comparison with the entire volume of PP. Moreover, deep coloring of PP remains a challenging issue.

Among the chemical modifications of PP, sulfonation has been paid considerable attention. The structure and mechanism of PP sulfonation have been studied with various sulfonating agents, including fuming sulfuric acid,²³ hot concentrated sulfuric acid,^{24,25} gaseous SO₃,²⁶ and liquid-phase reactions via a solution containing SO₃.²⁷ However, the main focus of these studies has been adhesion promotion^{24,26–29} and the investigation of an ion-exchange membrane³⁰ rather than dyeability.

Sulfonic acid is one of the most hydrophilic anions apart from metals and metal salts.³¹ Dyeing is usually performed in an aqueous solution. If the substrates can be swollen by water, such as wool, silk, and cotton, the dye molecules can be diffused into the polymer effectively. Therefore, the gain of hydrophilicity by the incorporation of sulfonic acid to PP can be an extra benefit for the dyeability.

In this work, a preparation scheme for bulk-modified PP is presented. In this scheme, chlorinated polypropylene (Cl-PP) is used as a source material that enables bulk modification in most organic solvents. Sulfonated polypropylene (SPP) has been prepared in two steps: substitution of chloride by thiol followed by successive oxidation to the sulfonate

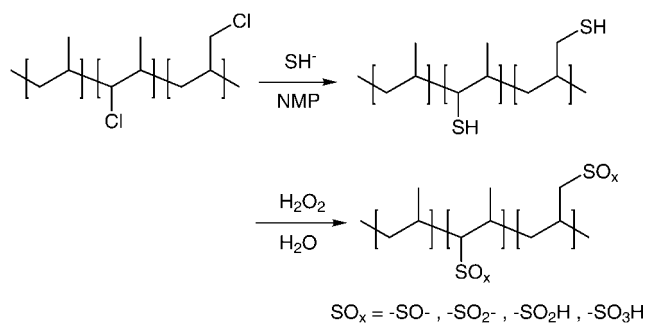


Figure 1 Reaction scheme for the preparation of SPP from Cl-PP.

(Fig. 1). The advantages of this two-step method over the direct sulfonation of Cl-PP are discussed in detail. Although the synthesis of thiol from alkyl halide³² and oxidation of thiol to sulfonic acid^{33–37} are well-known reactions, the incorporation of thiol into a PP template has not been reported to date, and the oxidation pathway of polymeric thiol has not been fully revealed. The dyeability of SPP to a basic dye is also presented.

EXPERIMENTAL

Thiol substitution reaction of Cl-PP

The reaction procedure for thiol substitution was as follows. Seven grams of purified Cl-PP (55.2 mmol of chlorine in the case of 28% chlorine content) and 450 mL of *N*-methyl-2-pyrrolidone (NMP) were placed in a 500-mL jacketed reactor and then dissolved to clearness at 85°C with stirring. The solution was cooled to room temperature without stirring being stopped, and a certain amount of a 40 wt % sodium hydrosulfide aqueous solution (78.5 mmol of SH in the case of an 11-g feed) was added slowly. Sodium hydrogen sulfide was purchased in a hydrate form, and its concentration was determined by titration.³⁸ The reactor was heated with circulating water, and the temperature was controlled at a specific temperature such as 85°C. After 3 h or another reaction time, the jacketed reactor was cooled with circulating cooling water. The solution was centrifuged for 20 min at 3500 rpm. After the removal of the upper layer of the NMP solution, the remaining precipitate was redispersed in distilled water, filtered with a 0.45-μm cellulose nitrate membrane filter, washed with distilled water, and dried in a 60°C vacuum oven for 12 h. A white-to-yellow powder was obtained. When the thiolated product was oxidized readily, the products were simply dispersed into distilled water without a vacuum-drying procedure. Products were kept in a dark place to prevent the formation of thyl radicals by UV. A Raman analysis was carried out on a Bruker

RFS1000 FT-Raman spectrometer with a 100-mW 1064-nm light source and a resolution of 4 cm^{-1} . Samples in powder or pressed sheet forms were used for the Raman analysis.

In each experiment, the hydrosulfide-to-chlorine ratio ($[\text{SH}^-]_0/[\text{RCl}]_0$) could be calculated from the initial dose of hydrosulfide and the chlorine content in Cl-PP. Elemental analyses were carried out with an Elementar GmbH Vario EL elemental analyzer. Sulfur and chlorine contents were calculated from the elemental analysis results and could be expressed as molar ratios with respect to carbon atoms. The chlorine–thiol substitution ratio (S_{Cl}) and hydrosulfide conversion (C_{SH}) were calculated as follows:

$$S_{\text{Cl}} (\%) = 100 \times \frac{S/C}{\text{Cl}/C} \quad (1)$$

$$C_{\text{SH}} (\%) = \frac{[\text{RSH}]}{[\text{SH}^-]_0} = \frac{[\text{RCl}]_0 \times S_{\text{Cl}}}{[\text{SH}^-]_0} \quad (2)$$

where S/C is the sulfur-to-carbon molar ratio in the thiolated PP, Cl/C is the chlorine-to-carbon molar ratio in Cl-PP, $[\text{RSH}]$ is the substituted thiol concentration in the product, $[\text{SH}^-]_0$ is the initial concentration of hydrosulfide ions, and $[\text{RCl}]_0$ is the initial concentration of chloride in the polymer.

Oxidation of thiolated PP

The thiolated PP was dispersed in distilled water, and oxidation was accomplished by the addition of a 35% hydrogen peroxide solution at 80°C. Three moles of hydrogen peroxide was needed to oxidize 1 mol of thiol to sulfonic acid; the molar ratio of hydrogen peroxide to thiol in thiolated PP ($\text{H}_2\text{O}_2/\text{SH}$) was controlled from 3.0 to 9.4. The suspension pH was varied from 4.0 to 10.0 with a buffer solution, and mere distilled water was used in the case of uncontrolled pH. The product was transferred and filtered with a 0.45- μm cellulose nitrate membrane filter, washed with distilled water, and dried in a 60°C vacuum oven for 24 h. As a result, 0.89–1.02 g of oxidized products was obtained from 1.0 g of thiolated PP; these values correspond to a 78–91% product yield if the yield is calculated on the basis of the theoretical quantity (i.e., all thiol in thiolated PP is converted to sulfonic acid). Each sample was mixed with KBr and pressed into a disc. The infrared spectrum was recorded on a Jasco FT/IR-470 Plus with a 4- cm^{-1} resolution, baseline-corrected, and normalized to the peak at 1458 cm^{-1} , which corresponded to asymmetric deformation of C–H in the methyl group and $-\text{CH}_2-$ scissor vibration.

The water uptake of an oxidized sample was measured to express the degree of hydrophilicity. Sheet samples were prepared by hot pressing to an

approximately 280- μm thickness at 160°C. Samples were weighed and immersed in distilled water at 70°C for 24 h. Surface water was wiped away, and the sheets were quickly weighed to obtain the water absorption. The water uptake was calculated from the ratio of the weight gain to the original sheet according to the following equation:

$$\text{Water uptake (\%)} = \frac{W_{\text{wet}} - W_{\text{dry}}}{W_{\text{dry}}} \times 100 \quad (3)$$

where W_{wet} and W_{dry} are the weights of wet and dried sheets, respectively.

Dyeability tests

A staining liquor was prepared by the dissolution of a dye in distilled water (0.1–4.2 g/L) and the addition of a pH 4.5 acetic acid buffer solution for the dyeability test of SPP. The acetic acid buffer strength of the staining liquor was maintained at 100 mM. Dyeing was performed on the powder form and hot-pressed sheet form, weighed samples were put into each vial, and the staining liquor was added. The staining liquor to sample ratio was kept at 40 : 1 (g/g). Staining was performed for 1 h in a 90°C water bath. After the staining was finished, each vial was cooled to room temperature, and the upper staining liquor was decanted and washed with distilled water and ethanol until the washed solution was clear.

The dyestuff used in the experiment was highly soluble in ethanol; the dye molecules adsorbed on the surface were washed out in this step. The used staining liquor and washed solution were collected together sample by sample and then diluted to a proper concentration to determine the dye concentration with an ultraviolet–visible spectrophotometer. The dye concentration was calculated with a precalibrated curve with the known concentration of the dye solution. From the initial and final quantities of dye in the liquor, the dye-uptake ratio was calculated as follows: dye-uptake ratio = $(C_i - C_f)/C_i$, where C_i is the initial dye content in the staining liquor before staining and C_f is the final dye content remaining in the liquor after staining. Washed sample sheets were dried at room temperature for 1 day. Total reflectance of the sheet was measured with a Varian Cary 100 ultraviolet–visible spectrophotometer with a Lab Sphere DRA-CA-3300 accessory and a 8° wedge. The K/S value was calculated from the reflectance with the following Kubelka–Munk equation:³⁹

$$\frac{K}{S} = \frac{(1 - R)^2}{2R} \quad (4)$$

where K is the absorption coefficient, S is the scattering coefficient, and R is the reflectance.

RESULTS AND DISCUSSION

Advantages of the two-step method for sulfonation

A two-step method for sulfonation from Cl-PP was investigated. In terms of the preparation of the dyeable PP, this approach can offer several advantages over the direct sulfonation of PP or Cl-PP. The first advantage is the retardation of a side reaction, which is somewhat related to the sulfonation position and an elimination problem. During the sulfonation of PP, the formation of a double bond by elimination of sulfonic acid is a frequently reported side reaction. When the secondary or tertiary sulfonic acid is eliminated, double bonds are formed in the main chain. The nearby tertiary carbon acquires additional stability by allylic resonance and will then readily accept SO_3 . By repetition of SO_3 addition and desulfonation, conjugated double bonds are formed, leading to the formation of dark-colored products.²⁷ In the case of a sulfonation reaction on solid PP, restriction of the conformational change forces the sulfonation position onto primary and tertiary carbons rather than to a secondary position.²⁵ However, in the solution reaction of Cl-PP, there is no strain to direct sulfonation to the primary position; thus, the formation of a conjugated double bond is a vital issue.

This problem can be resolved, to a certain extent, by separation of the addition reaction and elimination reaction. Hydrosulfide is a good nucleophile, and the reactivity of nucleophilic substitution depends on the position (primary > secondary > tertiary) of the chlorine atom. Primary thiol is a major product; its oxidation product gives primary sulfonic acid. Although primary sulfonic acid is eliminated during the oxidation reaction, the resulting double bond is isolated; it does not produce a conjugated double bond as eliminated H_2SO_3 is not sufficiently reactive in water to be re-added to the main chain. This effect appears in the color of the product. The product here is white to pale yellow, whereas a product with conjugated double bonds is often brown to dark brown.

The second advantage is a better sulfonation yield. The yield of the direct sulfonation of Cl-PP can be poor. Tada and Ito²⁵ proposed a model for surface sulfonation of solid PP involving an electrophilic addition of SO_3 . Kaneko and Sato⁴⁰ suggested another mechanism in their sulfonation of a PP film with fuming sulfuric acid, in which a $\text{C}=\text{C}$ double bond is formed first by hydride abstraction by SO_3 and the subsequent loss of a proton. SO_3 then undergoes electrophilic addition to form a double bond. In both mechanisms, electron-rich carbon atoms play a key role in the addition step. The carbon atoms in Cl-PP become electron-deficient because of the inductive effect of nearby chlorine atoms. If the sulfo-

nation of Cl-PP occurs, the reaction intermediates are thereby destabilized, and SO_3 addition or hydride abstraction becomes unfavorable; this results in a poor sulfonation yield.

Electron deficiency is no more an issue in nucleophilic substitution as chloride can be substituted by hydrosulfide with a good yield. Moreover, a higher yield of sulfonation can be expected in comparison with a direct method. As for the direct sulfonation of PP, it is difficult to estimate the conversion of SO_3 ; an excess amount of the sulfur source (concentrated H_2SO_4 , SO_3 , or fuming sulfuric acid) is necessary nonetheless to modify the surface of PP. However, in these experiments, a reasonable hydrosulfide conversion is achieved, such as 70% conversion for 3.5 mmol/g of sulfur and 45% conversion for 5.5 mmol/g of sulfur.

The third advantage is easy control of the degree of sulfonation. When hot concentrated sulfuric acid or fuming sulfuric acid is used with PP, it is difficult to estimate the exact sulfur trioxide concentration released from the reagents. Furthermore, because of the high reactivity of the reagent, the reaction proceeds to the end within a few minutes to 30 min; it is difficult to terminate the reaction at the designed degree of sulfonation. In contrast, thiolation takes place under mild conditions; hydrosulfide can be substituted quantitatively with chloride. Thus, it is possible to control the degree of substitution, regardless of the content, whereas the maximum substitution is limited by the chlorine content in Cl-PP.

Thiolation of Cl-PP

The substitution of thiol was confirmed by a Raman analysis. The general range for the thiol characteristic peak is 2600–2540 cm^{-1} .⁴¹ In the IR spectrum, the $-\text{S}-\text{H}$ stretching vibration peak is exceedingly weak and somewhat overlaps with the vibration peak of pure PP. Thus, a Raman analysis is more useful for identifying the thiol group. Cl-PP shows three sharp peaks of the $-\text{C}-\text{Cl}$ stretching vibration at 727, 707, and 687 cm^{-1} . As thiolation proceeds, the peaks at 727 and 687 cm^{-1} disappear, and the intensity of the 707- cm^{-1} peak decreases. In addition, a $-\text{S}-\text{H}$ stretching peak at 2584 cm^{-1} forms (Fig. 2). These three chlorine vibration peaks can also be observed at the same wave number in the Fourier transform infrared (FTIR) spectra: the peak at 727 cm^{-1} is close to the wave number of poly(allyl chloride) in ref. ⁴² at 730 cm^{-1} , which corresponds to the primary chlorine vibration peak. The band around 1660 cm^{-1} is thought to reflect the formation of a $\text{C}=\text{C}$ double bond due to the elimination of hydrogen chloride. Among the peaks of thiolated PP, 1458, 1380, and 975 cm^{-1} are from PP, and 1154 and 807 cm^{-1} are from Cl-PP.

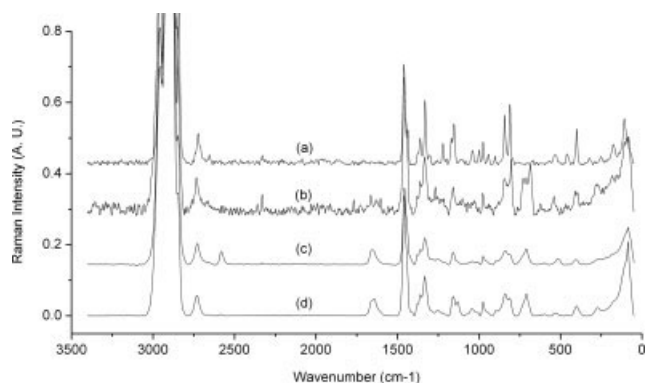


Figure 2 Raman spectra: (a) PP, (b) Cl-PP, (c) thiolated PP, and (d) SPP.

Figure 3 shows the reaction time dependence of S_{Cl} . Two reaction rate scales can be observed: the first is fast (<30 min), and the second is slow (>24 h). S_{Cl} increases sharply at the beginning of the reaction within 30 min. This is thought to be due to the substitution of primary chlorine, which is the major substituted product in nucleophilic substitution. The disappearance of the 727-cm^{-1} peak clearly supports this postulate. The subsequent slow and steady increase of S_{Cl} is thought to be due to substitution of secondary chlorine. The intensity of the 707-cm^{-1} peak depends on the reaction conditions; the sample with a larger S_{Cl} value showed lower intensity. As the major chlorine positions of the received Cl-PP were identified as being primary and secondary by $^{13}\text{C-NMR}$ (the spectrum is not shown), and the vibration intensity of tertiary chlorine is weak in general, tertiary chlorine was not observed in the vibronic spectrum. As the reaction temperature increased, the S_{Cl} values increased. For the reaction

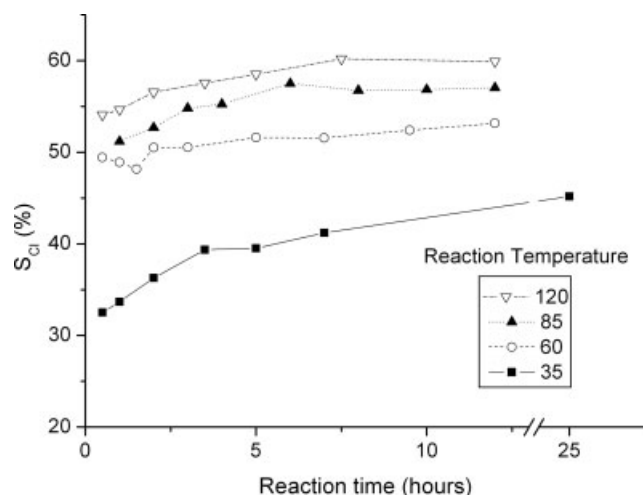


Figure 3 S_{Cl} versus the thiolation reaction time according to the reaction temperature. In each set of reactions, $[\text{SH}^-]_0/[\text{RCl}]_0$ is equal to 1.5.

temperature, 85°C is appropriate, although a higher chlorine substitution ratio was obtained at 120°C . However, some degree of degradation occurs at 120°C , resulting in a lower product yield, and the color of the product turns from white-yellow to red-brown. Furthermore, S_{Cl} does not increase significantly. Thus, a reaction time of 3 h was applied in the following experiments.

S_{Cl} and C_{SH} values are shown with the concentration dependence of $[\text{SH}^-]_0/[\text{RCl}]_0$ in the reagent in Figure 4(a,b). The thiol content incorporated in this experiment corresponds to 1.7–14.7% sulfur for 28% Cl-PP and 4.2–20.5% sulfur for 32% Cl-PP. As the initial hydrosulfide concentration increases, S_{Cl} linearly increases until $[\text{SH}^-]_0/[\text{RCl}]_0$ is below 0.6 for 28% Cl-PP and 0.7 for 32% Cl-PP. At higher $[\text{SH}^-]_0/[\text{RCl}]_0$ values, S_{Cl} deviates from linearity and eventually shows saturation behavior. The slope of the fitting line does not depend on the initial chlorine content of Cl-PP, but the maximum S_{Cl} value is

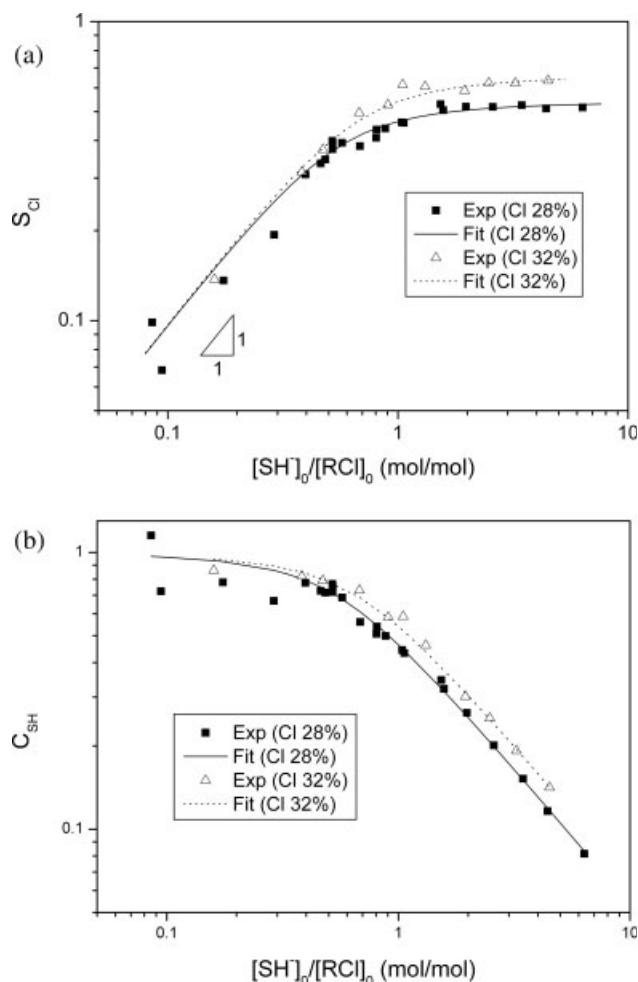


Figure 4 (a) S_{Cl} and (b) C_{SH} in the thiolation reaction. Experimental data for the thiolation of (■) 28% Cl-PP and (△) 32% Cl-PP and corresponding theoretical curves with fitted parameters are presented.

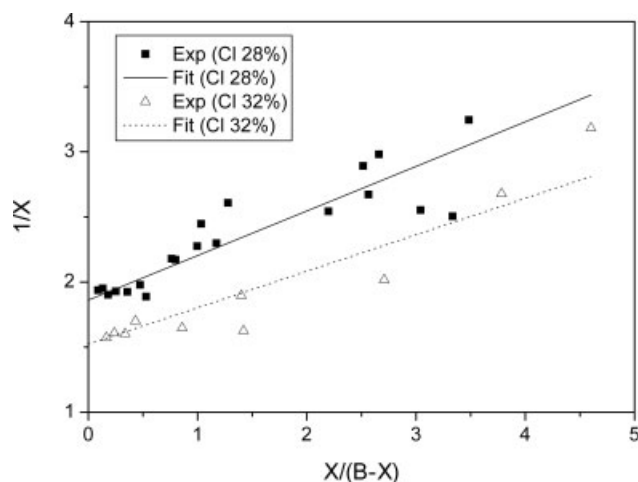
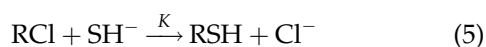


Figure 5 Determination of the parameters of the thiolation reaction. Thiolation data for (■) 28% Cl-PP and (△) 32% Cl-PP and their least-square fitting lines are presented.

increased as the chlorine content is increased from 28 to 32%. This behavior can be understood under the assumption that the substitution reaction is governed by the equilibrium condition:



Under this reaction condition, only some of the chlorine is substituted, even with excessive SH, and it seems reasonable to assume that chlorine is divided into two groups. The first group of chlorine is exchangeable with hydrosulfide, and the substitution ratio depends on the equilibrium condition. For instance, most of them are thought to be primary chlorine. The second group of chlorine does not readily exchange or has a slow rate of reaction at a given temperature. Thus, it can be considered constant throughout the reaction timescale. With some mathematical work, S_{Cl} can then be expressed as a function of S_m , K , and $[\text{SH}^-]_0/[\text{RCI}]_0$, where S_m is the ratio of chlorine involved in the reaction in a given timescale and K is the equilibrium constant. These parameters can be determined from experimental data. Fitting parameters and the derivation of the equation are given in the third section of the appendix. Through the plotting of $1/X$ versus $X/(B-X)$ (where X is equal to S_{Cl} and B is equal to $[\text{SH}^-]_0/[\text{RCI}]_0$), S_m and K can be determined from the reciprocal of the intercept and intercept over the slope, respectively:

$$\frac{1}{X} = \frac{1}{K \cdot S_m} \cdot \frac{X}{B-X} + \frac{1}{S_m} \quad (6)$$

The experimental data in an X and B form and the least-square lines for 28 and 32% Cl-PP are shown in

Figure 5. The 28% Cl-PP and 32% Cl-PP have the same thiolation reaction environment. It is reasonable to assume that they share the same equilibrium constant K . The common K value and two S_m values for each Cl-PP are calculated from the least-square fitting: $S_m(28\% \text{ Cl}) = 0.537$, $S_m(32\% \text{ Cl}) = 0.657$, and $K = 5.4$. The theoretical curves with these parameters are shown in Figure 4(a,b). An interesting feature is the initial slope in the $S_{\text{Cl}}-[\text{SH}^-]_0/[\text{RCI}]_0$ plot. As shown in the third section of the appendix, the initial slope always reaches unity and does not depend on S_m or K . This fact fits well with the experimental observations. With this model, it is possible to calculate the amount of hydrosulfide needed to prepare a designed quantity of sulfur in SPP, regardless of the reaction scale.

Oxidation of thiolated PP

The oxidation of thiol can be monitored with FTIR analysis (Fig. 6). Among the vibration peaks, sulfonic acid peaks were compared with the results of another group.²⁷ The peaks of the sulfur oxides in PP have not been reported thus far, and the peaks were assigned on the basis of the general vibration range of each moiety⁴¹ and the evolution behavior of the peaks during oxidation. These sulfur oxide peaks are summarized in Table I.

The assignment of sulfur oxide peaks proceeded as follows. The band due to the S—O stretching vibration can be found over a wide frequency range of 1330–1010 cm^{-1} as the vibration is influenced by the electronegativity of the attached group. During the oxidation of thiolated PP, peaks at 1039 and 1075 cm^{-1} appeared in the early stage of oxidation, and

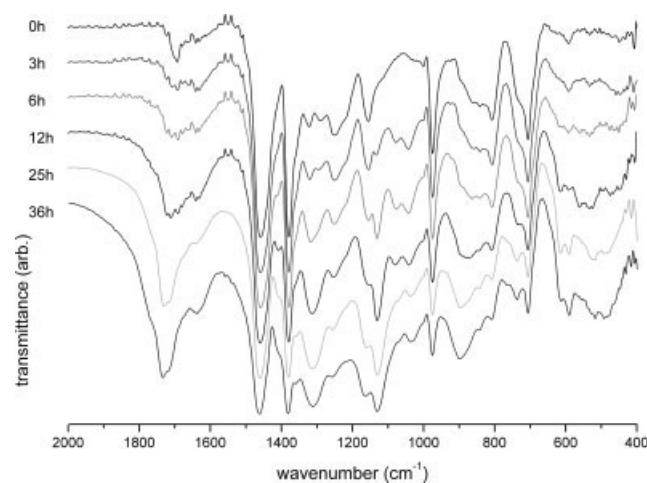
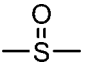
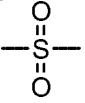
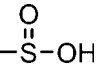
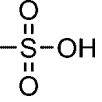


Figure 6 Changes in FTIR spectra with the oxidation time from 0 to 36 h. Thiolated PP with a sulfur content of 3.48 mmol/g was oxidized. The $\text{H}_2\text{O}_2/\text{SH}$ molar ratio was 8.3, and the H_2O_2 concentration was 0.52M. The peak height was normalized to the 1458- cm^{-1} peak and shifted.

TABLE I
Summary of Vibration Peaks

Functional group	Expected band (cm ⁻¹) ^a	Vibration mode ^a	Peak found (cm ⁻¹)
Sulfoxide 	1060–1010 730–660	vs S=O str (Raman m-w) v C–S str (Raman m-s)	1039 (s) —
Dialkyl sulfone 	1330–1290 1160–1120 790–700 600–480 520–430	vs asym SO ₂ str vs sym SO ₂ str (Raman s, p) m-s C–S str (Raman s) m-s SO ₂ def w-m SO ₂ wag	1311 (vs) 1130 (vs), (Raman 1133) 740 (w) — —
Sulfinic acid 	1090–990 870–810	vs S=O str (Raman m-s) m-s S–O str	1075 900–820, broad
Alkyl sulfonic acid 	1230–1120 (1160) ^b 1120–1025 (1040) (880) (580)	vs asym SO ₃ str s-m sym SO ₃ str S–O–C str SO ₂ def or C–S str	1163 Overlap with 1039 899, broad 590

asym, asymmetric; def, deformation; m-w, medium to weak; m-s, medium to strong; p, polarized; s, strong; str, stretching; sym, symmetric; v, varies; vs, very strong; w-m, weak to medium; wag, wagging.

^a The general ranges of expected bands and vibration modes are from ref. 41.

^b The wave numbers shown in parentheses are those of SPP in ref. 27.

strong peaks at 1311 and 1130 cm⁻¹ then increased (Fig. 6). Through another set of experiments, it was confirmed that the 1039-cm⁻¹ peak appears first and that the 1075-cm⁻¹ peak and a broad —OH stretching peak at 3400 cm⁻¹ then appear together. Among these S—O vibration peaks, only 1130 cm⁻¹ shows a significant increase in the Raman spectrum, whereas the 1039-, 1075-, and 1130-cm⁻¹ peaks do not. In the Raman spectrum, the symmetric S—O vibration mode from sulfone is strong, whereas the S—O vibration mode of sulfoxide is weak. According to the simultaneous growth of peaks in the middle stage of oxidation, 1311 and 1130 cm⁻¹ are from sulfone, and the Raman spectrum confirms that 1130 cm⁻¹ should be assigned to the symmetric S—O vibration peak of sulfone. The peak at 1039 cm⁻¹ is not accompanied by —OH stretching and is assigned as the S—O vibration peak of sulfoxide. Finally, the peak at 1075 cm⁻¹ is assigned as the peak of sulfinic acid.

It should be noted that the sulfoxide peak (1039 cm⁻¹) overlaps with the symmetric S—O stretching of sulfonic acid. It was not possible to confirm the presence of sulfoxide after the sulfonic acid had formed.

It is interesting that sulfinic acid was detected at the early stage of oxidation. According to the literature, peroxides oxidize the thiol by two pathways.³⁴ One involves the formation of disulfide in the first step, with the subsequent formation of sulfoxide, sulfone, sulfinic acid, and sulfonic acid in the following step. The second pathway involves the direct for-

mation of sulfinic acid through an unstable sulfenic acid (R—SOH) intermediate. Additionally, in the case of the oxidation of thiol by hydrogen peroxide, the initially formed product is in most cases the corresponding disulfide. Once disulfide forms, the formation of sulfinic acid is after that of sulfone. In these experiments, the presence of sulfinic acid before sulfone is possibly due to the restricted mobility of thiol bound to the polymer chain. If the thiol environment is hindered by a hydrocarbon chain, the thiol has a low probability of meeting another thiol. By accepting 2 mol of peroxide before meeting another thiol, it can follow the sulfinic acid pathway instead of the disulfide pathway. The sulfinic acid peak, 1075 cm⁻¹, disappears with the formation of sulfonic acid. The peaks at 1163, 899, and 590 cm⁻¹ in the spectrum of a reaction of 25 h (shown in Fig. 6) correspond to the peaks of SPP as sulfonated by concentrated sulfuric acid.²⁷

The band around 1642 cm⁻¹ is thought to be from the C=C double bond, and the broad band around 1712 cm⁻¹ is thought to be C=O from carboxylic acids and ketones, which are the oxidation products of the double bond. The origin of the double bond is likely the elimination of hydrogen chloride or sulfonic acid. It was found that although the S/C ratio in the polymer does not show significant differences, these bands continuously grow from the beginning. Thus, it is possible to conclude that the major contribution here is dehydrohalogenation. The effect of desulfonation on this band is discussed at the end of this section.

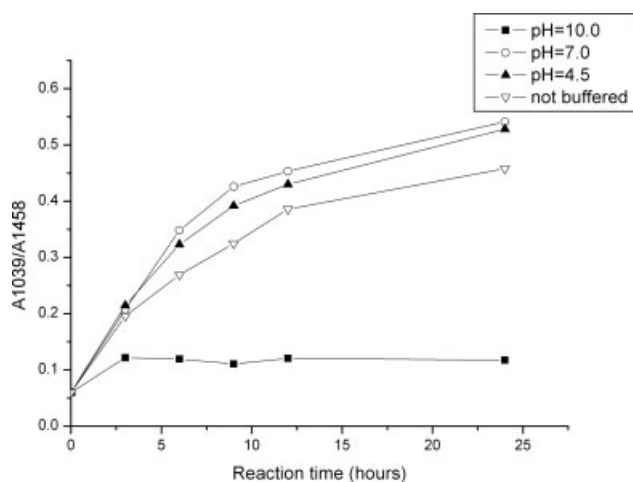


Figure 7 pH dependence of the oxidation of thiolated PP. The peak of sulfoxide (1039 cm^{-1}) is plotted against the oxidation time. The sulfur concentration in the thiolated PP was 4.0 mmol/g . The reaction conditions were as follows: 80°C , $[\text{H}_2\text{O}_2]/[\text{RSH}] = 3.3$, and $[\text{H}_2\text{O}_2] = 0.2\text{M}$.

The pH dependence of the oxidation reaction was examined, as shown in Figure 7. With the oxidation of monomeric thiol by hydrogen peroxide, the rate of the reaction (r) is known to be proportional to the hydrogen peroxide concentration and is inversely proportional to the square root of the hydrogen-ion concentration:³⁴

$$r = k[\text{H}_2\text{O}_2]/[\text{H}^+]^{1/2}$$

However, it was found that overly rapid decomposition of hydrogen peroxide produces less oxidized product in this system, as shown in Figure 7. At pH 10, only a sulfoxide peak (1039 cm^{-1}) appears, and other moieties such as sulfinic acid or sulfone are not observed. An iodine test of the reaction solution after 6 h revealed that peroxide is already used up at this point. As oxidation proceeds, the reaction medium pH nearly reaches 1 at the end of the oxidation process in an unbuffered solution. However, the initial slope shows only a slight difference between pH 7.0, pH 4.5, and an unbuffered solution.

The oxidation reaction conditions and results are summarized in Table II. The S/C ratio shows that the oxidation of thiol was completed successfully with a small decrease in the sulfur content; however, with a high dose of hydrogen peroxide ($\text{H}_2\text{O}_2/\text{SH} = 8.3\text{--}9.4$), a significant amount of sulfur (22–38%) was eliminated (experiments 3-7 and 3-8).

In the normalized IR spectrum, the intensity level of 1039 cm^{-1} ($-\text{SO}-$), 1130 cm^{-1} ($-\text{SO}_2-$), 1168 cm^{-1} ($-\text{SO}_3\text{H}$), and 1712 cm^{-1} ($\text{C}=\text{O}$) represents the relative concentration of each moiety. However, it should be noted that the S–O vibration peaks are broad and too close to overlap, and this makes it difficult to

TABLE II
Summary of the Oxidation Reactions^a

Experiment	$[\text{H}_2\text{O}_2]$ (M)	$\text{H}_2\text{O}_2/\text{RSH}$ (mol/mol)	Reaction time (h)	Sulfur in TPP (mmol of sulfur/ mol of carbon) ^b	Sulfur in SPP (mmol of sulfur/ mol of carbon)	Water			IR absorbance		
						uptake (%)	A_{1039}	A_{1130}	A_{1712}		
3-1	0.50	3.0	24 h	47	46	3.2	0.18	0.22	0.03		
3-2	0.36	3.3	24 h	61	58	4.2	0.26	0.43	0.12		
3-3	0.37	3.3	24 h	71	70	31	0.53	0.87	0.29		
3-4	0.44	3.3	52 h	67	60	11	0.32	0.96	0.34		
3-5	0.33	4.6	24 h	80	73	18	0.49	0.89	0.26		
3-6	0.40	7.1	48 h	48	45	68	0.31	0.83	0.37		
3-7	0.52	8.3	36 h	63	49	21	0.39	0.97	0.53		
3-8	0.77	9.4	24 h	72	52	124	0.87	1.21	0.85		

^a The pH of the suspension was not controlled. The reaction temperature was 80°C .

^b TPP = thiolated polypropylene.

use them quantitatively as an extent of oxidation. The absorbance at 1712 cm^{-1} (A_{1712}) increases steadily as oxidation proceeds; this is considered here as the relative extent of oxidation.

Water-uptake properties are associated with the wettability of a polymer. This is essential for the quick and uniform wetting of fabric. The groups of samples with 70–80 mmol of sulfur/mol of carbon in thiolated PP show 11–31% water uptake after oxidation (experiments 3-3, 3-4, and 3-5). However, with a high dose of hydrogen peroxide ($\text{H}_2\text{O}_2/\text{RSH}$) and a longer oxidation time, the sample shows a greater extent of oxidation ($A_{1712} = 0.85$) and a considerable water-uptake increase (experiment 3-6).

The dyeability of the SPP can be influenced by desulfonation and a loss of the water-uptake property. The samples that experience severe sulfur elimination during oxidation (experiments 3-5 and 3-7) show relatively low levels of water uptake in comparison with a sample with a similar sulfur content (experiments 3-3 and 3-6), except for an exceptional case with a high extent of oxidation (experiment 3-8). The major contribution of the decrease in the sulfur content here appears to be desulfonation as sulfonic acid is a good leaving group, whereas the other sulfur oxide intermediates (e.g., disulfide, sulfoxide, and sulfone) are not. In addition, this explains the relatively low level of water uptake of the desulfonated sample; the water-absorbing ability is largely dependent on the acid moiety, especially sulfonic acid.

Dyeability

SPP shows strong affinity to a basic dye, and modification is effective in enhancing the dyeability of PP. Figure 8 shows the dye-absorbing behaviors of Cl-PP and three SPP samples for different sulfur contents. To determine the maximum dye-binding capacity, a broad range of dye concentrations, 0.03–0.14 g of dye/g of polymer, was applied. SPP shows very good affinity to a basic dye. Until dye binding is saturated, it shows a dye-uptake ratio of 99%. It should be noted that this high uptake ratio was measured after an ethanol wash. The dissolving power of ethanol is strong enough to wash out loosely bound dye molecules from the substrate surface. It is believed that this high degree of dyeability results from the strong ionic interaction between the sulfonate and basic dye and from the contribution of the bulk modification.

The SPP with a higher sulfur oxide modification level has a higher maximum dye-binding capacity. For instance, the dye uptake reaches 190 mmol of dye/kg of polymer for SPP of 3.6 mmol of sulfur/g of polymer at a dye concentration of 0.11 g of dye/g of polymer. This value corresponds to 52.8 mmol of

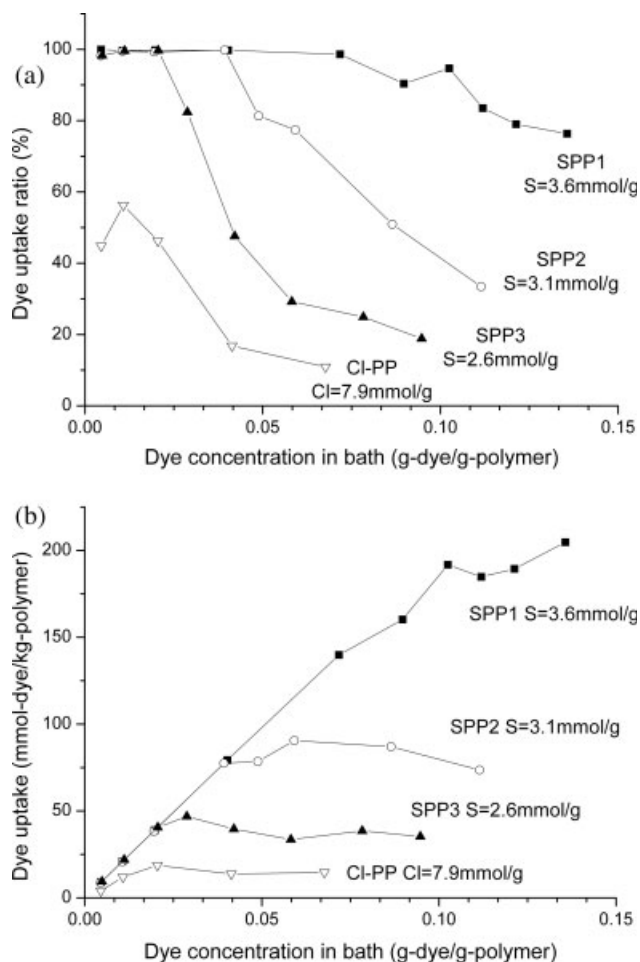


Figure 8 Dye-absorbing behaviors of Cl-PP and SPPs with different sulfur concentrations. Dyeing was performed on the powder form of the samples.

dye/mol of sulfur; it is over 20 times more effective than that of Cl-PP, which has only a small capacity of 2.5 mmol of dye/mol of chlorine.

The maximum binding capacity for fibers can be found in the literature.^{1,43} Nylons have 25–55 mmol/g for an acid dye, and wool has approximately 900 mmol/kg for an acid dye. Pristine PP has only 0.1–0.3 mmol of dye/kg for a disperse dye. For cationic dyes, acrylic fiber has 36–58 mmol/kg, and the dye exhaustion of cationically dyeable poly(ethylene terephthalate) is only 25–50% of the acrylic fiber value. Recently, Bhattacharya and Inamdar¹⁹ grafted poly(acrylic acid) with a graft add-on of approximately 30%. They achieved satisfactory dyeability with basic dyes, which was comparable to that with cationically dyeable poly(ethylene terephthalate). However, modification with sulfonic acid has been shown to be more beneficial for dye-uptake efficiency and the level of dye saturation in comparison with acrylic acid.

SPP in sheet form was stained with a basic dye, and the K/S values were compared with that of Cl-

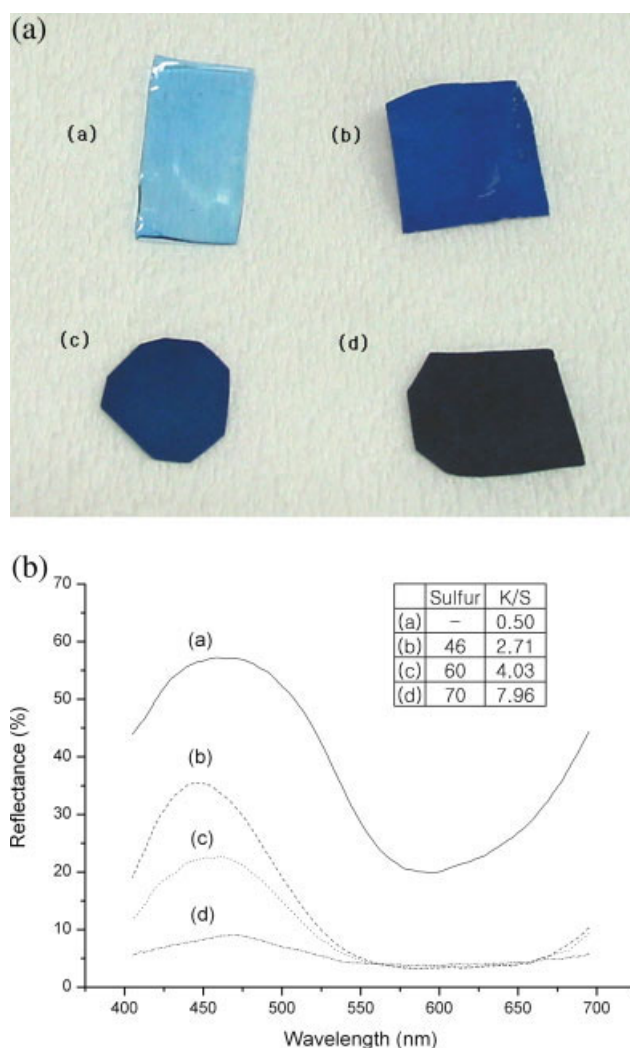


Figure 9 Photography and reflectance of basic dye-stained sheets: (a) Cl-PP and (b–d) SPP. The inset shows the sulfur content (mmol of sulfur/mol of carbon) and K/S value. The staining conditions were as follows: dye/sample ratio = 0.011, sample/liquor = 1:40, and staining for 1 h at 90°C. [Color figure can be viewed in the online issue, which is available at www.interscience.wiley.com.]

PP (Fig. 9). In this experiment, the reflectance of SPP at 592 nm reached the minimum; therefore, average values over 400–700 nm were used instead. As the sulfur content increased, a deeper blue color was achieved.

SPP can be stained with disperse dyes, although they are less effective than basic dyes. SPP with 3.9 mmol of sulfur/g of polymer was dyed with Disperse Orange 3, and 25% dye uptake was achieved for 2% depth of shade. Disperse dye absorption was related not only to the sulfur content but also to the extent of oxidation; a less oxidized sample could show better dyeability to the disperse dye. A comprehensive investigation is needed to understand the dyeing behavior with disperse dyes.

From a practical point of view, the chlorine content of received Cl-PP and the extent of sulfonation are rather high to be applied directly to dyeable PP applications. However, we believe that our method offers an excellent potential candidate for dyeable PP and other purposes as well by using a lower chlorine content for Cl-PP and adjusting the sulfur level.

CONCLUSIONS

SPP was prepared from Cl-PP via thiolation and successive oxidation to improve the dyeability of PP. Through the reaction of Cl-PP in the solution, functional groups could be incorporated through the PP chain, rather than solely on the surface. This reaction scheme, consisting of a two-step process, has a number of advantages over direct sulfonation. It is controllable and sufficiently reactive, and it suppresses desulfonation and the formation of conjugated double bonds.

The effects of the reaction time, temperature, and hydrosulfide concentration on the chlorine–thiol substitution and hydrosulfide conversion for the optimal processing conditions were examined. As the dose of hydrosulfide increases, the substitution of chlorine to thiol linearly increases when the hydrosulfide-to-chlorine ratio is low. In addition, it shows saturation behavior, which can be explained with an equilibrium model between hydrosulfide and accessible chlorine at a given timescale. At a higher reaction temperature, a higher substitution ratio is achieved. A temperature of 85°C was found to be suitable for both substitution and for minimizing product loss.

The oxidation reaction of thiolated PP was investigated with FTIR and Raman analyses. The evolution of oxidation intermediates was examined in detail. Sulfinic acid in the early stage of oxidation was observed, and it was concluded that the limited mobility of thiol could increase the likelihood of the formation of sulfinic acid instead of following the disulfide pathway. The extent of oxidation was discussed in terms of reaction parameters such as the pH, dose of hydrogen peroxide, and thiol content. The relationship between the water uptake and the extent of oxidation was also discussed.

SPP showed strong affinity to a basic dye, and modification was found to be effective for enhancing the dyeability of PP. A maximum dye uptake of 190 mmol of dye/kg of polymer was achieved.

In short, by the use of thiol as a functionalization template of PP, it was possible to incorporate aliphatic sulfonic acid into PP for dyeable PP. As thiol has important characteristics, such as a special affinity with gold⁴⁴ and expandability by a thiol–ene reaction,⁴⁵ the use of a thiolated polymer is expected to provide a new and efficient method to functionalize

PP for common and other purposes, some of which are under consideration in the laboratory.

The authors thank Won Lee for the idea of dyeable PP and for consistent encouragement and assistance.

APPENDIX

Materials used in this study

American Chemical Society reagent grade NMP and sodium hydrosulfide were obtained from Aldrich Chemical. EP-S electronic-grade 2-propanol was obtained from Dongwoo Fine Chemicals (Korea). Other solvents such as methanol, acetone, cyclohexane, and diethyl ether were extrapure-grade and were obtained from DC Fine Chemicals (Korea) or Junsei Chemicals (Japan). These solvents were used without further purification. The 35% aqueous solution of hydrogen peroxide was extrapure-grade and was obtained from Junsei Chemicals. The dyestuff, basic blue 26 (Victoria Blue B), was American Chemical Society reagent grade and was obtained from Aldrich Chemical. Cl-PPs having (1) a molecular weight of about 100,000 mol/g and a chlorine content of 28% or (2) a molecular weight of about 150,000 mol/g and a chlorine content of 32% were obtained from Aldrich Chemical.

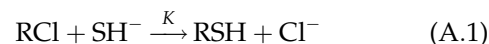
Purification of Cl-PP

Cl-PP (40 g) was dissolved with stirring in 400 mL of cyclohexane at 70°C for at least 3 h. The solution was cooled to room temperature and then centrifuged (3500 rpm for 20 min). The upper translucent solution was collected in a 1000-mL beaker. Methanol (400 mL) was slowly added to the collected solution with stirring. The solution was then left without stirring until the polymer solution phase was separated. The upper methanol layer was drained off, and the solution was poured into 1000 mL of 2-propanol. The precipitated polymer was sliced (1–2 mm thick) and then dried in a 60°C vacuum oven for 48 h. Purification was confirmed by the disappearance of peaks at 1510, 1182, and 760 cm^{-1} in the FTIR spectrum. The chlorine content in Cl-PP was measured via elemental analysis.

Equilibrium model of thiolation

Expressions of S_{Cl} and C_{SH}

Consider the equilibrium in the thiol substitution reaction [eq. (A.1)]. The initial concentration of chloride is $[\text{RCl}]_0$, but only parts of chlorine atoms can participate in the reaction; assume that the initial concentration of available chloride is $S_m[\text{RCl}]_0$. Let x be the equilibrium advancement at time t ; the concentrations of the substances are given by eq. (A.3):



At time = 0

$$S_m[\text{RCl}]_0 \quad [\text{SH}^-]_0 \quad (\text{A.2})$$

At time t

$$S_m[\text{RCl}]_0 - x \quad [\text{SH}^-]_0 - x \quad x \quad (\text{A.3})$$

The equilibrium constant can be written as

$$K = \frac{x^2}{(S_m[\text{RCl}]_0 - x)([\text{SH}^-]_0 - x)} \quad (\text{A.4})$$

Here we define new variables for convenience:

$$X = \frac{x}{[\text{RCl}]_0} = \frac{[\text{RSH}]}{[\text{RCl}]_0} = S_{\text{Cl}} \quad (\text{A.5})$$

$$B = \frac{[\text{SH}^-]_0}{[\text{RCl}]_0} \quad (\text{A.6})$$

where X is the chlorine–thiol substitution ratio and B is the hydrosulfide-to-chlorine ratio in the reagent. Dividing both the divisor and dividend of eq. (A.4) by $([\text{RCl}]_0)^2$ and substituting eq. (A.5) and eq. (A.6), we find that K becomes

$$K = \frac{X^2}{(S_m - X)(B - X)} \quad (\text{A.7})$$

$$(K - 1)X^2 - K(B + S_m)X + KS_mB = 0 \quad (\text{A.8})$$

This is a second-order equation with respect to X and can be solved as follows:

$$X(S_m, K, B) = \begin{cases} \frac{S_m + B}{2} \frac{K}{K - 1} \pm \sqrt{\left(\frac{S_m + B}{2}\right)^2 \cdot \frac{K^2}{(K - 1)^2} - S_m \cdot B \cdot \frac{K}{K - 1}} & (-) \text{ for } K > 1, \quad (+) \text{ for } K < 1 \\ \frac{S_m \cdot B}{S_m + B} & \text{for } K = 1 \end{cases} \quad (\text{A.9})$$

C_{SH} is by definition

$$C_{SH} = \frac{[RSH]}{[SH^-]_0} = \frac{x}{[SH^-]_0} = \frac{x/[RCl]_0}{[SH^-]_0/[RCl]_0} = \frac{X}{B} \quad (A.10)$$

Hence, dividing eq. (A.9) by B , we have

$$C_{SH}(S_m, K, B) = \begin{cases} \left(\frac{1 + S_m/B}{2} \right) \frac{K}{K-1} \pm \sqrt{\left(\frac{1 + S_m/B}{2} \right)^2 \cdot \frac{K^2}{(K-1)^2} - \frac{S_m}{B} \cdot \frac{K}{K-1}} & (-) \text{ for } K > 1, \quad (+) \text{ for } K < 1 \\ \frac{S_m}{S_m + B} & \text{for } K = 1 \end{cases} \quad (A.11)$$

Derivation of the fitting equation

The equation for the fitting can be derived from eq. (A.7). The equation is arranged as follows:

$$K(S_m - X) = \frac{X^2}{B - X} \quad (A.12)$$

$$K \cdot S_m = \frac{X^2}{B - X} + KX \quad (A.13)$$

Dividing both side by $1/KXS_m$ gives

$$\frac{1}{X} = \frac{1}{K \cdot S_m} \cdot \frac{X}{B - X} + \frac{1}{S_m} \quad (A.14)$$

Initial slope in the $S_{Cl^-}[SH^-]_0/[RCl]_0$ plot

In the region of small $[SH^-]_0/[RCl]_0$, both X and B are small quantities. Since S_m is a constant, $O(1)$, if we ignore higher order terms of X and B , X^2 and XB , the eq. (A.8) becomes

$$-KS_mX + KS_mB = 0 \quad (A.15)$$

This implies $X = B$; the slope is unity.

References

- Dathy, K. V.; Vaidya, A. A. *Chemical Processing of Synthetic Fibers and Blends*; Wiley: New York, 1984.
- (a) Tategami, Y.; Nishihara, H.; Kobayashi, Y.; Shinonaga, H. Jpn. Pat. 085844 (1978); (b) Omae, T.; Murakami, M.; Nishihara, H.; Shinonaga, H. Jpn. Pat. 159455 (1979).
- (a) Sheth, P. J.; Chandrashekar, V.; Kolm, R. R. U.S. Pat. 5,550,192 (1996); (b) Nakamura, H.; Tokimitsu, T.; Koshirai, A. Jpn. Pat. 292659 (2004).
- Tamano, H. Jpn. Pat. 074143 (1984).
- Akrman, J.; Prikryl, J. *J Appl Polym Sci* 1996, 62, 235.
- Dayioglu, H. *J Appl Polym Sci* 1992, 46, 1539.
- Teli, M. D.; Adivarekar, R. V.; Ramani, V. Y.; Sabale, A. G. *Fibers Polym* 2004, 5, 264.
- Son, T. W.; Lim, S. K.; Chang, C. M.; Kim, S. S.; Cho, I. S. *J Soc Dyers Colourists* 1999, 115, 366.
- (a) Fan, Q. G.; Ugbole, S. C.; Wilson, A. R.; Dar, Y. S.; Yang, Y. Q. *AATCC Rev* 2003, 3, 25; (b) Fan, Q.; Yang, Y.; Ugbole, S. C.; Wilson, A. R. U.S. Pat. 6,646,026 B2 (2003); (c) Mani, G.; Fan, Q. G.; Ugbole, S. G.; Eiff, I. M. *AATCC Rev* 2003, 3, 22.
- Fujie, H.; Funekawa, S. Jpn. Pat. 003429 (1996).
- Dominguez, R. J. G.; Henkee, C. S.; Crawford, W. C.; Cummings, G. W.; Hess, K. J.; Clark, R. J.; Evans, R. K. U.S. Pat. 5,985,999 (1999).
- Mizutani, Y.; Nago, S.; Kawamura, H. *J Appl Polym Sci* 1997, 63, 133.
- Chan, C. M. *Polymer Surface Modification and Characterization*; Hanser/Gardner: Munich, 1994.
- Tokita, T.; Inagaki, H. Jpn. Pat. 018098 B2 (1995).
- Kanazawa, H. Jpn. Pat. 090783 (1995).
- Zhang, D.; Spence, P. D.; Sun, Q.; Wadsworth, L. C. U.S. Pat. 6,479,595 B1 (2002).
- Kim, H. J.; Shtanko, H. I.; Lim, Y. J.; Lee, K. P. *J Korean Soc Dyers Finishers* 2003, 15, 44.
- Bondar, Y. V.; Kim, H. J.; Lim, Y. J. *J Appl Polym Sci* 2007, 104, 3256.
- Bhattacharya, S. D.; Inamdar, M. S. *J Appl Polym Sci* 2007, 103, 1152.
- Borsig, E. *J Mater Sci Pure Appl Chem* 1999, 36, 1699.
- Sharma, D. N.; Samanta, A. K. *Text Trends* 1990, 33, 35.
- Samanta, A. K.; Sharma, D. N. *Indian J Fibre Text Res* 1995, 20, 206.
- Tehrani, A. R.; Shoushtari, A. M.; Malek, R. M. A.; Abdous, M. *Dyes Pigments* 2004, 63, 95.
- Cameron, G. G.; Main, B. R. *Polym Degrad Stab* 1983, 5, 215.
- Tada, H.; Ito, S. *Langmuir* 1997, 13, 3982.
- Asthana, H.; Erickson, B. L.; Drzal, L. T. *J Adhes Sci Technol* 1997, 11, 1269.
- Cameron, G. G.; Main, B. R. *Polym Degrad Stab* 1985, 11, 9.
- Chikh, R. B.; Askeland, P. A.; Schalek, R. L.; Drzal, L. T. *J Adhes Sci Technol* 2002, 16, 1651.
- Ericson, B. L.; Asthana, H.; Drzal, L. T. *J Adhes Sci Technol* 1997, 11, 1249.
- Compan, V.; Fernandez-Carretero, F. J.; Riande, E.; Linares, A.; Acosta, J. L. *J Electrochem Soc B* 2007, 154, 159.
- Kim, K. J.; Lee, J. M. *Chemistry of Dyeing*, 2nd ed.; Hyeong-Seol: Seoul, 1990; p 207.
- Trofimov, B. A.; Petrova, O. V.; Vasiltsov, A. M.; Korzhova, S. A.; Mikhaleva, A. I.; Skotheim, T. A.; Kovalev, I. P.; Mikhailik, Y. V. *Sulfur Lett* 2000, 23, 297.
- Block, E. *Reactions of Organosulfur Compounds*; Academic: New York, 1978.

34. Capozzi, G.; Modena, G. In *The Chemistry of the Thiol Group*; Patai, S., Ed.; Wiley: Chichester, England, 1974; Part 2, p 785.
35. Noller, C. R.; Gordon, J. J. *J Am Chem Soc* 1933, 55, 1090.
36. Vivian, D. L.; Reid, E. E. *J Am Chem Soc* 1935, 57, 2559.
37. Wallace, T. J.; Schriesheim, A. *Tetrahedron* 1965, 21, 2271.
38. (a) Jensen, K. A.; Rasmussen, O. V. *Z Anal Chem* 1933, 94, 180; (b) Song, W.; Ai, H.; Zhang, Y. *Huafei Gongye* 2003, 30, 48.
39. (a) Kubelka, P.; Munk, F. *Z Tech Phys* 1931, 12, 593; (b) Kubelka, P. *J Opt Soc Am* 1948, 38, 448.
40. Kaneko, M.; Sato, H. *Macromol Chem Phys* 2005, 206, 456.
41. Socrates, G. *Infrared and Raman Characteristic Group Frequencies*, 3rd ed.; Wiley: Chichester, England, 2001.
42. Murahashi, S.; Nozakura, S.; Hatada, K. *Bull Chem Soc Jpn* 1961, 34, 631.
43. Peters, R. H. *Textile Chemistry*; Elsevier Scientific: New York, 1975; Vol. III.
44. Witt, D.; Klajn, R.; Barski, P.; Grzybowski, B. A. *Curr Org Chem* 2004, 8, 1763.
45. Hoyle, C. E.; Lee, T. Y.; Roper, T. J. *J Polym Sci Part A: Polym Chem* 2004, 42, 5301.